Assessment of Choroidal Vascularity and Choriocapillaris Blood Perfusion in Anisomyopic Adults by SS-OCT/OCTA

Hao Wu,[1–3] Guoyun Zhang,[1–3] Meixiao Shen,[1–3] Renchang Xu,[1–3] Pengqi Wang,[1–3] Zhenqi Guan,[1–3] Zhu Xie,[1–3] Zi Jin,[1–3] Sisi Chen,[1–3] Xinjie Mao,[1–3] Jia Qu,[1–4] and Xiangtian Zhou[1–4]

[1]Eye Hospital and School of Optometry and Ophthalmology, Wenzhou Medical University, Wenzhou, Zhejiang, China
[2]State Key Laboratory of Optometry, Ophthalmology and Vision Science, Wenzhou, Zhejiang, China
[3]National Clinical Research Center for Ocular Diseases, Wenzhou, Zhejiang, China
[4]Research Unit of Myopia Basic Research and Clinical Prevention and Control, Chinese Academy of Medical Science, Wenzhou, Zhejiang, China

PURPOSE. To explore the association of choroidal vascularity and choriocapillaris blood perfusion with myopic severity in anisomyopes.

METHODS. Refractive error, axial length (AL), and other biometric parameters were measured in 34 anisomyopic young adults. Macular choroidal thickness (ChT) and choroidal vascularity, including total choroidal area (TCA), luminal area (LA), stromal area (SA), and choroidal vascularity index (CVI), were determined from swept-source optical coherence tomography (SS-OCT) vertical and horizontal B-scans. The percentage of choriocapillaris flow voids (FV%) was obtained from en face SS-OCT-angiography.

RESULTS. The spherical equivalent refraction (SER) was –3.35 ± 1.25 diopters in the more myopic eyes and –1.25 ± 1.17 diopters in the less myopic eyes ($P < 0.001$). The interocular difference in SER was highly correlated with that in AL ($P < 0.001$). The macular ChT, TCA, LA, and SA were smaller in the more myopic eyes than in the less myopic eyes in both vertical and horizontal scans (all $P < 0.001$). Importantly, the CVIs in vertical and horizontal scans were smaller and the FV% was greater in the more myopic eyes ($P < 0.05$). In vertical scans, the interocular difference in CVIs was correlated with that in the SER, AL, and ChT (all $P < 0.05$). The interocular difference in FV% was correlated with that in SER, AL, and vertical and horizontal ChTs (all $P < 0.05$).

CONCLUSIONS. Choroidal vascularity and choriocapillaris blood perfusion were lower in the more myopic eyes of anisomyopic adults. These changes were correlated with the severity of myopia and choroidal thinning, indicating that choroidal blood flow is disturbed in human myopia.

Keywords: choroidal vasculature, choriocapillaris, anisomyopia, myopia, optical coherence tomography

$\mathbf{M}$yopia is one of the most common visual disorders worldwide. It has been estimated that the global prevalence of myopia will increase from 33.9% in 2020 to 49.8% in 2050, with the prevalence of high myopia increasing from 5.2% to 9.8%.[1] Myopia, particularly high myopia, is characterized by excessive axial elongation and increased risk of developing a series of complications,[2–4] such as degenerative retinopathy, lacquer cracks, choroidal neovascularization, and posterior staphylomas. All of these conditions contribute to irreversible visual impairment, with serious economic and social consequences.[5] Therefore, it is imperative to study the risk factors for myopia development.

In recent years, clinical studies using optical coherence tomography (OCT) have demonstrated that choroidal thinning accompanies the development of myopia, and a close association has been established between choroidal thickness changes and ocular growth.[6–12] Observations in animal models of myopia have shown that choroidal thinning occurs early in myopia development, preceding the longer term acceleration of ocular growth, and, conversely, that choroidal thickening accompanies the slowing of ocular growth.[13–16] These bidirectional changes in choroidal thickness may be attributable to changes in choroidal blood flow (ChBF), with a positive correlation between them.[17–19] Considering the highly vascularized nature of the choroid and its potential role in scleral hypoxia,[20] we proposed that decreases in ChBF are responsible for the development of human myopia.[19,20]

OCT is a non-invasive, high-resolution, in vivo imaging technique. In combination with OCT-angiography (OCTA), the information of choroidal vasculature and choriocapillaris blood perfusion could be obtained simultaneously for the assessment of ChBF.[21] This technique has been applied in studies on high or pathologic myopic adults. In those

eyes, both choroidal vascular luminal area (LA) and stromal area (SA) were reduced,[22] and the area of choriocapillaris flow voids (FVs) was increased, indicating diminished areas with perfusion.[23] However, the accompanying pathological changes, such as extreme choroidal thinning or choroidal atrophy, would make it difficult to determine whether the changes in choroidal parameters are associated with myopia itself or with myopia-related pathological changes.

Therefore, to clearly define the associations between ChBF and myopia, in the present study we used swept-source (SS)-OCT/OCTA to perform a comprehensive analysis of choroidal vasculature and choriocapillaris blood perfusion in anisomyopic adults who were not highly myopic (spherical equivalent refraction [SER] > –6.00 D) in both eyes. Anisomyopic individuals have an interocular difference in myopic SER of at least 1.00 D. This condition is typically due to an interocular asymmetry in axial length, usually due to differences in vitreous chamber depth (VCD).[24] Comparison of the more myopic eye to the less myopic fellow eye, within the same anisomyopic individual, allows for greater control of potentially confounding inter-subject variables such as age, gender, and genetic and environmental factors. Thus, this model should provide increased sensitivity in detecting abnormalities in the variables of interest, and the associations among them, in low to moderate human myopia.

METHODS

Subjects

Thirty-four college student participants, 20 to 27 years old, were recruited from Wenzhou Medical University from September 2019 to July 2020. Written informed consent was obtained from all participants. The study was approved by the ethics committee of the Eye Hospital of Wenzhou Medical University. All participants were treated in accordance with the tenets of the Declaration of Helsinki.

Ophthalmic screening examinations, including non-cycloplegic subjective refraction, binocular testing, ocular health evaluation, and intraocular pressure measurement, were conducted prior to formal enrollment. All subjects were anisomyopes with an interocular difference in SER of at least 1.0 D. The subjects were free of ocular and systemic disease and had best-corrected visual acuities of 0.00 logMAR or better in each eye. None had a history of ocular surgery, smoking, or systemic diseases. Subjects were asked to avoid caffeine and alcohol intake during the 24 hours before choroidal imaging.

Ocular Biometric Measurements

Following the screening, the participants were directed to watch a 20-minute video on a television at a distance of 5 meters with their full-distance spectacle corrections to eliminate the effect of any previous visual stimuli on the choroid, such as high accommodation[25] or defocus.[26,27] The choroidal images were taken immediately after this period by SS-OCT/OCTA, as detailed below. Ocular biometric parameters, including corneal radius (CR), central corneal thickness (CCT), anterior chamber depth (ACD), lens thickness (LT), and axial length (AL), were measured using the Lenstar LS 900 (Haag Streit, Koeniz, Switzerland). The VCD was calculated as the AL – (CCT + ACD + LT). All of the

measurements were conducted from 13:30 to 17:00 to minimize any potential impact of diurnal variation.[28,29]

SS-OCT/OCTA Image Acquisition and Analysis

The SS-OCT/OCTA system (VG200S; SVision Imaging, Henan, China) contained a SS laser with a central wavelength of approximately 1050 nm and a scan rate of 200,000 A-scans per second. The system was equipped with an eye-tracking utility based on an integrated confocal scanning laser ophthalmoscope to eliminate eye-motion artifacts. The axial resolution was 5 μm, and lateral resolution was 13 μm. The scan depth was 3 mm.

Structural OCT of the macular region was performed with 18 radial scan lines centered on the fovea. Each scan line, generated by 2048 A-scans, was 12 mm long and separated from the adjacent lines by 10°. Sixteen B-scans were obtained on each scan line and were automatically averaged to improve the signal-to-noise ratio.[30] Only the vertical and horizontal scans were used to analyze the choroidal thickness and choroidal vascularity (Fig. 1A). Briefly, the choroid in the SS-OCT images was defined as the area from the retinal pigment epithelium (RPE)–Bruch's membrane complex to the choroid–sclera interface. After semiautomatic choroidal segmentation with a custom algorithm developed in MATLAB R2017a (MathWorks, Natick MA, USA), segmentations of RPE–Bruch's membrane complex and choroid–sclera interface were adjusted manually by a trained examiner (PW). The scan size was adjusted for the differences in magnification due to different ALs among the eyes. After segmentation, each image was binarized using custom-designed algorithms in MATLAB R2017a to demarcate the LA and SA with Niblack's autolocal threshold; this method was first proposed by Sonoda et al.[31] and further developed by Agrawal et al.[32] After image processing, the mean macular choroidal thickness (ChT), total choroidal area (TCA), LA, and SA were calculated. The choroidal vascularity index (CVI) was defined as the ratio of LA to TCA. The 6-mm macular region centered on the fovea was regarded as the region of interest.

For angiography, the choroidal images were obtained with a raster scan protocol of 512 horizontal B-scans that covered an area of 3 × 3 mm centered on the fovea. Each B-scan contained 512 A-scans and was repeated four times and averaged. The OCTA images were obtained by the SVision SS-OCTA algorithm. We evaluated en face angiograms of the choriocapillaris slab, which was defined by a layer starting at the basal border of the RPE–Bruch's membrane complex and ending at approximately 20 μm beneath the RPE–Bruch's membrane complex (Fig. 2A). A maximum projection was applied on the segmented volumes to generate the en face angiograms. Projection artifacts from retinal vessels were removed by the algorithm. FVs were defined as regions having no flow signals that were detectable by the threshold binarization algorithm, as previously described.[33] The FV percentage (FV%) was calculated by dividing the area of the FVs by the area of the measured region and then converting the value to percent. Because of poor image resolution at the scan edges, only the 2.5-mm-diameter circular region centered on the fovea was used for analysis.

According to the Early Treatment Diabetic Retinopathy Study (ETDRS) grid, the macular zone was divided into regions consisting of three concentric rings with diameters of 1 mm (central fovea, C), 3 mm (parafovea), and
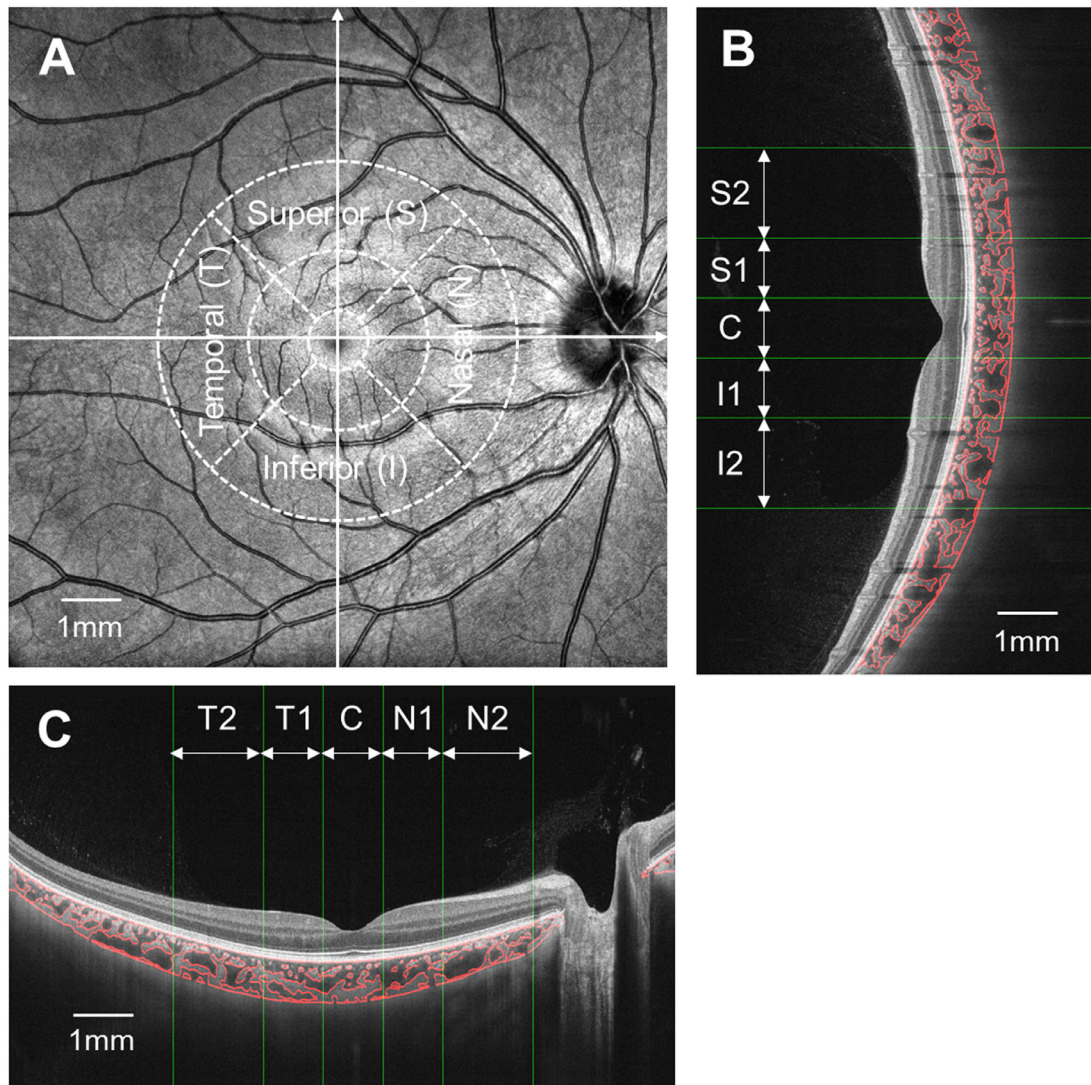
FIGURE 1. Illustration of choroidal vasculature analysis. (**A**) Macular ETDRS grid, (**B**) vertical scan, and (**C**) horizontal scan. Quadrants: I1, inferior parafovea; I2, inferior perifovea; S1, superior parafovea; S2, superior perifovea; T1, temporal parafovea; T2, temporal perifovea; N1, nasal parafovea; N2, nasal perifovea.

6 mm (perifovea). The parafoveal annulus (designated "1" in Figs. 1B, 1C) and perifoveal annulus (designated "2" in Figs. 1B, 1C) were further divided into superior (S1, S2), inferior (I1, I2), temporal (T1, T2), and nasal (N1, N2) quadrants (Fig. 1). This grid was applied to the vertical and horizontal B-scans (Figs. 1B, 1C), as well as the 2.5-mm-diameter region imaged for choriocapillaris angiography (Figs. 2B–2D).

To assess and affirm agreement within and between examiners, 22 eyes from 11 participants were selected, and the choroids were segmented twice by two trained examiners (PW and ZX). Intraclass correlation coefficients (ICCs) and coefficients of repeatability were calculated to assess the agreement of ChT, LA, SA, TCA, and CVI measurements within and between examiners at various regions. The coefficient of repeatability was calculated as 1.96 times the standard deviation of the differences between two measurements. After obtaining good agreement, all the scans were measured by examiner PW.

Statistics

The statistical analyses were performed using SPSS Statistics 23.0 (IBM, Armonk, NY, USA). The means and standard deviations of all continuous variables are presented unless otherwise stated. The normality of data was examined by the Shapiro–Wilk test. Paired t-tests or Wilcoxon signed-rank tests were used to assess the interocular differences between the fellow eyes for ocular biometrics, choroidal structural measurements, and choriocapillaris FV measurements. For topographic analysis to compare choroidal parameters between the fellow eyes, two-way repeated-measures (RM) ANOVAs were performed, including analysis for two within-subject factors (eyes and regions). The Greenhouse–Geisser correction was applied to the degrees of freedom when the sphericity assumption was violated. Bonferroni adjustments for multiple comparisons were applied to all post hoc pairwise comparisons. Pearson's or Spearman's correlation was used to calculate the degree and statistical significance of associations between variables wherever appropriate.
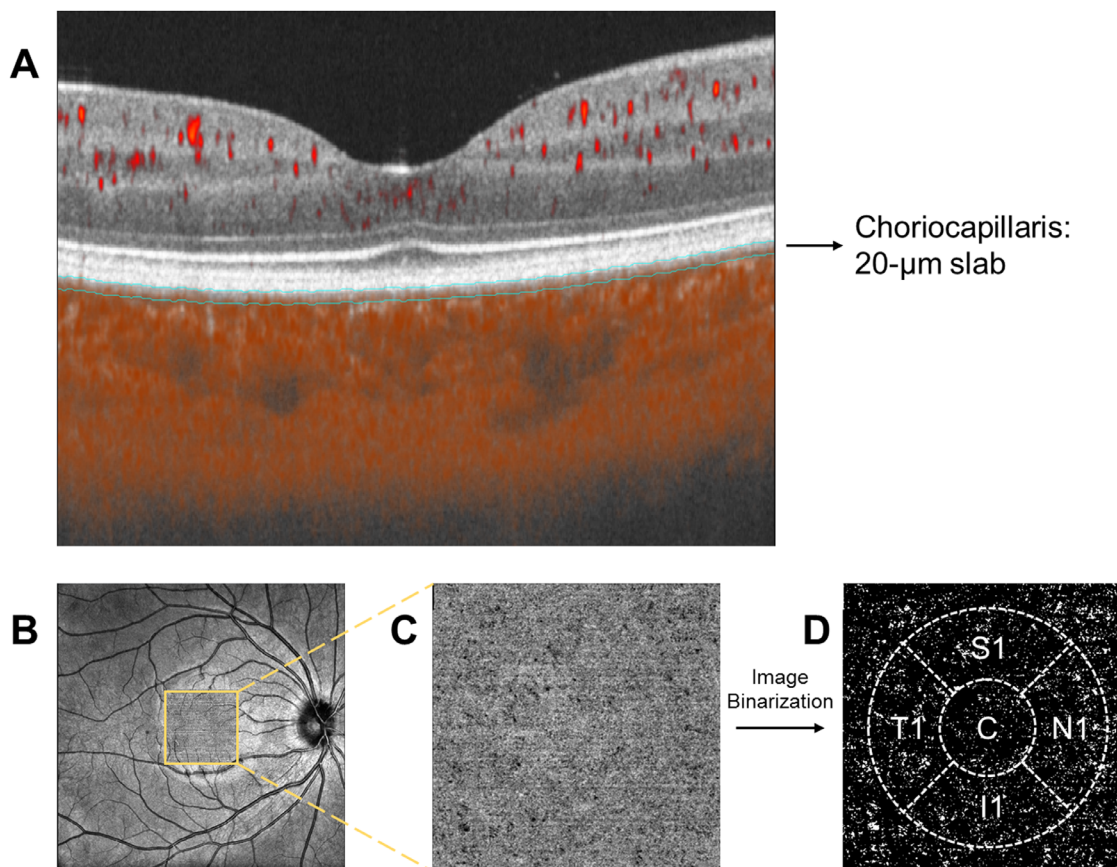
FIGURE 2. Illustration of choriocapillaris blood perfusion analysis. (**A**) Cross-sectional structure combined with flow OCT image with choriocapillaris segmentation lines. (**B**) OCTA scan region of 3 × 3 mm. (**C**) Magnified en face OCTA choriocapillaris image. (**D**) Inverted binarized images of FVs with the 2.5-mm ETDRS grid.

TABLE 1. Ocular Biometric Parameters of the Anisomyopic Participants

Parameter	Sample Size	More Myopic Eyes	Less Myopic Eyes	P
SER	34	−3.35 ± 1.25 D	−1.25 ± 1.17 D	<0.001[*]
CR	34	43.16 ± 1.40 D	43.11 ± 1.35 D	0.287[†]
VCD	33	17.80 ± 0.96 mm	16.95 ± 0.72 mm	<0.001[†]
AL	34	25.07 ± 0.94 mm	24.23 ± 0.71 mm	<0.001[†]

[*] P value determined by Wilcoxon signed-rank test.
[†] P value determined by paired t-test.

RESULTS

General Characteristics

Of the 34 participants included in the analyses, 10 were males and 24 were females, and the mean age was 23.4 ± 2.0 years old. The VCD for one subject was excluded from the final analysis because the measurement from the Lenstar A-scan did not exhibit a consistent visible peak from the posterior crystalline lens surface.

The SER of the more myopic eyes was −3.35 ± 1.25 D, and that of the less myopic eyes was −1.25 ± 1.17 D (P < 0.001) (Table 1). The AL in the more myopic eyes (25.07 ± 0.94 mm) was significantly longer than that in the less myopic eyes (24.23 ± 0.71 mm) (P < 0.001). The difference in AL was attributed mostly to the difference in VCD, which was 17.80 ± 0.96 mm in the more myopic eyes compared to

16.95 ± 0.72 mm in the less myopic eyes (P < 0.001). As expected, the magnitude of SER anisometropia was highly correlated with the interocular differences in VCD and AL (Spearman's correlation, r = −0.906 and r = −0.927 respectively; both P < 0.001).

Repeatability of Choroidal Structural Measurement

The ICC values of global and topographical ChT, LA, SA, TCA, and CVI varied from 0.89 to 0.99 for intra-examiner repeatability in vertical and horizontal scans (Supplementary Tables S1, S2). In the vertical and horizontal scans, the coefficients of repeatability within examiner varied from 10 to 32 µm for ChT, from 0.00 to 0.03 mm^2 for LA, from 0.01 to 0.07 mm^2 for SA, from 0.02 to 0.09 mm^2 for TCA,

TABLE 2. Global Choroidal Parameters in the More Myopic and Less Myopic Eyes of the Anisomyopic Participants ($n = 34$)

| Parameter | Mean ± SD | | P |
	More Myopic Eyes	Less Myopic Eyes	
ChT_V (μm)	306 ± 94	351 ± 88	<0.001[*]
ChT_H (μm)	271 ± 84	322 ± 86	<0.001[*]
LA_V (mm^2)	1.09 ± 0.35	1.27 ± 0.32	<0.001[*]
LA_H (mm^2)	0.96 ± 0.31	1.18 ± 0.34	<0.001[*]
SA_V (mm^2)	0.74 ± 0.22	0.83 ± 0.22	<0.001[*]
SA_H (mm^2)	0.66 ± 0.20	0.75 ± 0.19	<0.001[†]
TCA_V (mm^2)	1.84 ± 0.57	2.10 ± 0.53	<0.001[*]
TCA_H (mm^2)	1.62 ± 0.50	1.93 ± 0.51	<0.001[*]
CVI_V (%)	59.2 ± 3.2	60.5 ± 2.8	<0.01[†]
CVI_H (%)	59.0 ± 3.6	61.0 ± 3.3	<0.01[†]
FVs (%)	8.9 ± 2.0	8.0 ± 1.2	<0.05[†]

_V, vertical scan; _H, horizontal scan.
[*] P value determined by paired *t*-test.
[†] P value determined by Wilcoxon signed-rank test.

and from 1.9% to 5.0% for the CVI (Supplementary Tables S3, S4). Considering the means of these choroidal parameters, the repeatability of manual correction was good. The agreement between the examiners, as assessed by ICCs and coefficients of repeatability, was also good (Supplementary Tables S5–S8).

Global Analyses of Choroidal Vascularity and Choriocapillaris FVs

Both the vertical and the horizontal mean macular ChTs were significantly less in the more myopic eyes than in the less myopic eyes (both $P < 0.001$) (Table 2). There were also significant reductions in the vertical and horizontal LAs, SAs, and TCAs in the more myopic eyes compared to the less myopic eyes (all $P < 0.001$). Importantly, the CVIs of both the vertical and horizontal directions were also less in the more myopic eyes (both $P < 0.01$), and the percentage of FVs was greater in the more myopic eyes, as well ($P < 0.05$).

The interocular differences in LAs, SAs, and TCAs of both vertical and horizontal scans were significantly correlated with the interocular differences in SER, AL, and VCD (all $P < 0.01$) (Table 3). Additionally, the interocular differences in the CVIs of vertical scans were significantly correlated with interocular differences in SER, AL, and VCD (all $P < 0.05$). There were also significant correlations

between the interocular differences in FVs with SER, AL, and VCD (all $P < 0.01$). Furthermore, the interocular differences in ChTs were positively correlated with CVIs, LAs, SAs, and TCAs in both vertical and horizontal scans (all $P < 0.05$), and the interocular differences in FVs were negatively correlated with ChTs in the vertical and horizontal scans (both $P < 0.05$).

Topographic Analyses of Choroidal Vascularity and Choriocapillaris FVs

For vertical scans, the interaction effect of eyes and regions on ChT was significant (eyes × regions, $F = 3.88$, $P < 0.05$), as was the main effect of eyes on ChT (eyes, $F = 31.57$, $P < 0.001$). In vertical scans, the choroids in all regions were thinner in the more myopic eyes than in the less myopic eyes (all $P < 0.01$) (Fig. 3A). In horizontal scans, the main effects of eyes and regions on ChT were both significant (eyes, $F = 28.63$, $P < 0.001$; regions, $F = 102.28$, $P < 0.001$), whereas the interaction effect of eyes and regions on ChT was not significant. In all regions of horizontal scans, ChT was also significantly less in more myopic eyes than in less myopic eyes (all $P < 0.01$) (Fig. 3B).

Because the widths of the nine choroidal regions were different from one another (Fig. 1), the areas among them were not comparable; therefore, only the topographic areas between the fellow eyes were analyzed. The main effects of eyes on LA, SA, and TCA were all significant, in both the vertical scans (LA, $F = 30.74$, $P < 0.001$; SA, $F = 26.03$, $P < 0.001$; TCA, $F = 31.70$, $P < 0.001$) and horizontal scans (LA, $F = 31.92$, $P < 0.001$; SA, $F = 18.32$, $P < 0.001$; TCA, $F = 29.16$, $P < 0.001$). The LA (Figs. 4A, 4B), SA (Figs. 4C, 4D), and TCA (Figs. 4E, 4F) were significantly smaller in the more myopic eyes than in the less myopic eyes, in each region of both vertical and horizontal scans (all $P < 0.05$).

Importantly, the main effect of eyes on the CVI was significant in both vertical ($F = 8.31$, $P < 0.01$) and horizontal scans ($F = 13.94$, $P < 0.001$). The CVIs in the vertical scans of the I2 region (Fig. 5A) and in the horizontal scans of the T2, T1, C, and N2 regions (Fig. 5B) were significantly smaller in the more myopic eyes than in the less myopic eyes (all $P < 0.05$). However, there were no significant interaction effects of eyes and regions for the CVI, in vertical or horizontal scans.

The main effects of eyes and regions on the choriocapillaris FV% were both significant (eyes, $F = 5.88$, $P < 0.05$; regions, $F = 28.02$, $P < 0.001$), whereas the interaction effect

TABLE 3. Correlations Among the Interocular Differences in SER, AL, VCD, and Choroidal Parameters

Parameter	FVs	CVI_V	LA_V	SA_V	TCA_V	CVI_H	LA_H	SA_H	TCA_H
SER	**−0.443**[†]	**0.438**[†]	**0.629**[‡]	**0.509**[†]	**0.618**[‡]	0.258	**0.609**[‡]	**0.644**[‡]	**0.654**[‡]
AL	**0.499**[†]	**−0.359**[*]	**−0.591**[‡]	**−0.533**[†]	**−0.609**[‡]	−0.259	**−0.614**[‡]	**−0.657**[‡]	**−0.661**[‡]
VCD	**0.483**[†]	**−0.402**[*]	**−0.619**[‡]	**−0.526**[†]	**−0.631**[‡]	−0.247	**−0.605**[‡]	**−0.676**[‡]	**−0.659**[‡]
ChT_V	**−0.374**[*]	**0.482**[‖]	**0.978**[¶]	**0.919**[¶]	**1.000**[¶]	—	—	—	—
ChT_H	**−0.341**[*]	—	—	—	—	**0.407**[§]	**0.979**[¶]	**0.922**[¶]	**1.000**[¶]

Values are Spearman's or Pearson's correlation coefficients ($n = 34$ for SER, AL, ChT_V, and ChT_H; $n = 33$ for VCD). Interocular difference was defined as more myopic eyes minus less myopic eyes. Bold font indicates statistical significance.
[*] $P < 0.05$ by Spearman's correlation analysis.
[†] $P < 0.01$ by Spearman's correlation analysis.
[‡] $P < 0.001$ by Spearman's correlation analysis.
[§] $P < 0.05$ by Pearson's correlation analysis.
[‖] $P < 0.01$ by Pearson's correlation analysis.
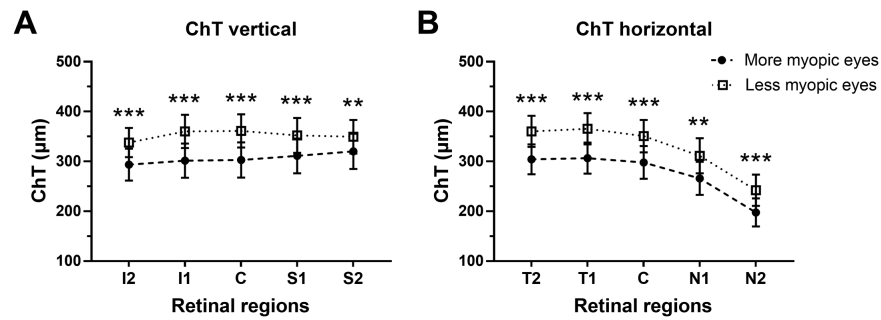[¶] $P < 0.001$ by Pearson's correlation analysis.

FIGURE 3. ChT topography in fellow eyes of anisomyopic subjects ($n = 34$). (**A**) ChT in vertical B-scans, (**B**) ChT in horizontal B-scans. Data are expressed as means and 95% confidence intervals. Two-way RM ANOVA; [**]$P < 0.01$ and [***]$P < 0.001$ indicate significant differences between the fellow eyes.
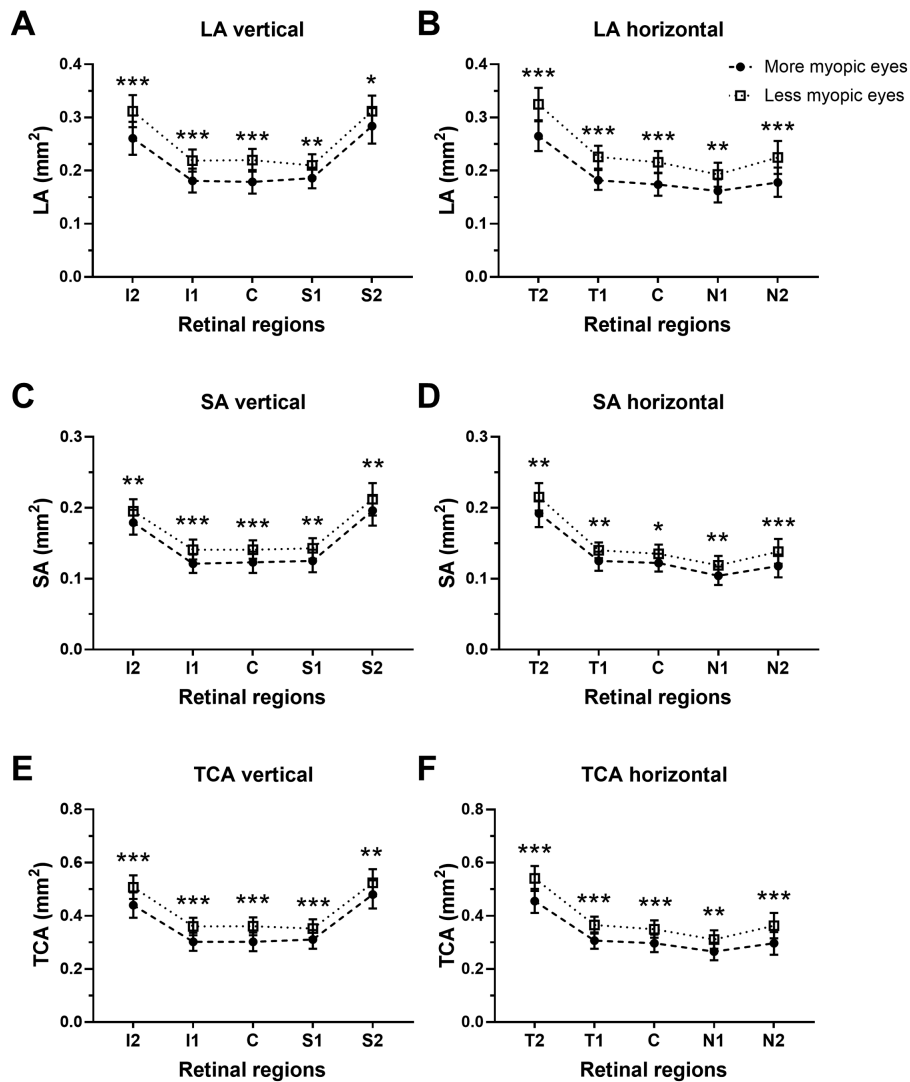

FIGURE 4. Topography of choroidal vascular components in fellow eyes of anisomyopic subjects ($n = 34$). (**A**) LA in vertical B-scans, (**B**) LA in horizontal B-scans, (**C**) SA in vertical B-scans, (**D**) SA in horizontal B-scans, (**E**) TCA in vertical B-scans, and (**F**) TCA in horizontal B-scans. Data are expressed as means and 95% confidence intervals. Two-way RM ANOVA; [*]$P < 0.05$, [**]$P < 0.01$, and [***]$P < 0.001$ indicate significant differences between the fellow eyes.
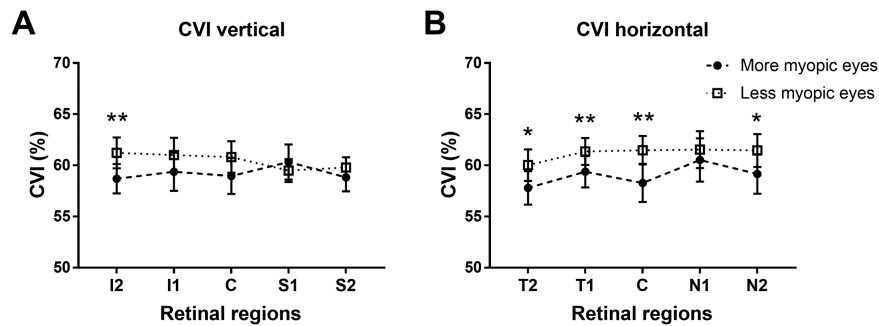
FIGURE 5. Topography of CVI in fellow eyes of anisomyopic subjects ($n = 34$). (**A**) CVI in vertical B-scans, and (**B**) CVI in horizontal B-scans. Data are expressed as means and 95% confidence intervals. Two-way RM ANOVA; $^*P < 0.05$ and $^{**}P < 0.01$ indicate significant differences between the fellow eyes.
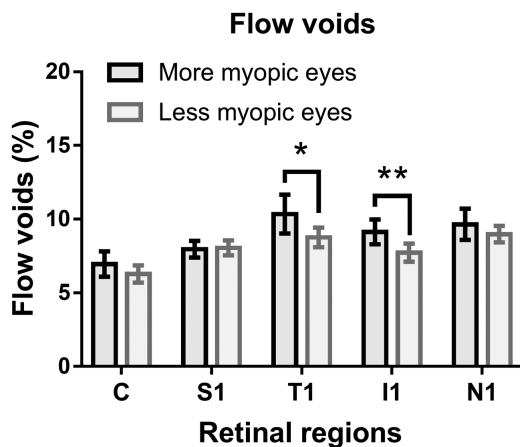

FIGURE 6. Topography of FVs in fellow eyes of anisomyopic subjects ($n = 34$). Data are expressed as means and 95% confidence intervals. Two-way RM ANOVA; $^*P < 0.05$ and $^{**}P < 0.01$ indicate significant differences between the fellow eyes.

of eyes and regions on FV% was not significant. In the T1 and I1 regions, FV% was greater in the more myopic eyes than in the less myopic eyes ($P < 0.01$) (Fig. 6).

DISCUSSION

The nature of the association between ChBF and myopia remains an urgent question. In this study, we performed comprehensive analyses of the choroidal vasculature and choriocapillaris blood perfusion in the disparate eyes of anisomyopic adults to test for an association between ChBF and myopia. The results showed that choroidal vascularity, assessed by SA, LA, TCA, and CVI, was lower in the more myopic eyes than in the less myopic eyes of anisomyopic subjects, whereas the choriocapillaris FV% was higher. Moreover, there were correlations between most of the choroidal parameters and severity of myopia, as indicated by SER, AL, and VCD. These findings indicate greater reductions in ChBF with greater degrees of myopia. In addition, the decrease in ChT was positively correlated with the decrease in choroidal vascularity and increases of choriocapillaris FVs, suggesting that the thinning of the ChT in myopia is associated with decreased ChBF.

Physiological Meaning of the Choroidal Parameters in SS-OCT/OCTA Images

The choroid consists of three vascular layers, designated (from the retinal side to the scleral side) as choriocapillaris, Sattler's layer, and Haller's layer. Sattler's layer contains medium to small vessels supplying discrete hexagonal lobules of capillaries in the choriocapillaris, and Haller's layer contains large vessels, providing the main arterial supply and venous drainage for the choroid.[34] Previous spectral domain-OCT[35,36] and SS-OCT[37,38] structural scans visualized vessel-like structures with low signal intensity and identified them as blood vessels. A limitation of this method is that, although medium- to large-size vessels could be visualized in that way, the visualization of small vessels was not possible because of limited lateral resolution and lack of contrast.[35,39–41] In OCTA en face images, the FVs, which appear as small dark regions, seem to represent the intercapillary spaces that are strikingly similar to those seen in morphological and histological images.[42,43] However, mainly because of signal attenuation attributed to scattering by RPE and choriocapillaris, OCTA cannot depict large vessels deep in the choroid.

To delineate the global appearance of choroidal circulation, we comprehensively analyzed the choroidal vascularity in structural OCT images and choriocapillaris FVs in OCTA images. The former reflects the circulatory volume in Haller's and Sattler's layers, and the latter reflect areas in the choriocapillaris with low perfusion or without perfusion, thus outlining the global choroidal circulation. These methods have shown good repeatability and reproducibility in studies by others,[32,33,42,44,45] as well as by us in the present work.

Gupta et al.[22] first reported reductions in choroidal LA and SA along with thinning of the ChT in high myopic eyes. Recently, Li et al.[45] used the same methodology in a population of low to moderately myopic children and reported negative correlations of LA with AL, but not with SER. On the other hand, several studies reported increased FVs in high myopic eyes, suggesting the presence of decreased choriocapillaris blood perfusion,[23,46] and Su et al.[46] did not find changes of FVs in moderately myopic eyes. By utilizing the special design of internal self-control in anisomyopes, we found that reductions in choroidal vasculature and choriocapillaris blood perfusion were positively correlated with the severity of myopia, as indicated by SER, AL, and VCD. Taken together, these studies suggest the presence of decreased choroidal circulation in human myopia.

It is noteworthy that topographical changes of CVIs and FVs in more myopic eyes were prominent in the temporal and inferior macular regions. A recent study reported that a strong accommodation stimulus (+6.00 D) could elicit a non-uniform reduction in choroidal thickness, with most prominent thinning in the temporal, inferior, and inferotemporal regions[25]; similar topographical variations were also observed in children after 3 weeks of orthokeratology treatment.[47] Nevertheless, only limited information has been obtained from the more peripheral choroid. Hoseini-Yazdi et al.,[48] working with a small sample size, reported that the magnitude of choroidal thinning was largest in the foveal region, diminishing gradually toward the more peripheral regions. In addition, studies in chicks showed greater choroidal thickening in the central region than in the peripheral region in response to myopic defocus.[49] These findings indicate that the central retinal (including macular) regions are particularly responsive to visual stimulus conditions, leading to a decrease in choroidal vascularity and choriocapillaris blood perfusion during myopia development.

Role of Choroidal Structure and Blood Flow During Myopia Development

In the past decade, OCT studies have clearly shown a close link between myopia and ChT[50] and that the ChT in myopic and high myopic eyes is thinner than in emmetropic and hyperopic eyes.[6–9] Recent longitudinal studies have further confirmed this link, showing that choroidal thinning is associated with accelerated ocular growth or myopia development in children and adolescents.[10–12] Our ChT measurements are consistent with those results. Recent studies found that the choroidal thinning in myopic eyes is mainly attributed to losses in Haller's and Sattler's layers.[51,52] The reductions in these two layers, in combination with the choroidal thinning and reduced choroidal vascularity that we found here, indicate that choroidal blood volume is reduced in myopic eyes.

Because the choriocapillaris is supplied by Sattler's and Haller's layers, changes in blood flow in these layers can be expected to disturb choriocapillaris blood perfusion. We observed an increase of choriocapillaris FVs in the more myopic eyes as compared to the less myopic eyes, and we found correlations of interocular differences in FVs with SER, AL, and ChT in both vertical and horizontal scans; other studies have also reported increased FVs in high myopic eyes.[23,46] Moreover, estimates of choroidal circulation, based on pulsatile ocular blood flow and ocular pulsation amplitude, were significantly lower in high myopes.[53–55] In addition, fundus indocyanine green angiography showed delayed choroidal filling in high myopic eyes.[56] Collectively, these studies indicate a close association between decreased ChBF and myopia severity in humans.

A key remaining unresolved need is to determine the cause-and-effect relationship between ChBF and myopia—that is, whether decreased ChBF causes myopia development, or vice versa. Early studies in form-deprived myopic chicks observed reductions in ChBF.[17] Upon removal of the form-deprivation diffuser, ChBF recovered within hours,[18] which is much more rapid than the alterations in scleral remodeling and ocular elongation. The bidirectional response of ChBF to visual cues, which determines the differential ocular elongation rate, was also demonstrated in our recent study using OCT/OCTA technology.[19] ChBF and ChT in guinea pigs were decreased after induction of myopia by form-deprivation or hyperopic defocus, and they recovered after removal of these altered optical conditions. Of note, actively increasing ChBF with vasodilator prazosin inhibited myopia progression in guinea pigs, as well as axial elongation and scleral hypoxia.[57] We have argued that a decrease in ChBF may cause scleral hypoxia followed by axial elongation and myopia.[20,58] Because the choroidal thickness in humans could also respond rapidly and predictably to various visual stimuli (e.g., hyperopic defocus, myopic defocus, and accommodation),[25–27] it is plausible that decreased ChBF is a risk factor for the development of human myopia.

Limitations of the Current Study

Due to the limitations of cross-sectional design, the current study can only further strengthen the association between the reduction in ChBF and myopia development. To test the hypothesis that decreased ChBF is a risk factor for the clinical development of myopia, longitudinal studies are needed. Another limitation of this study is that our evaluation of choriocapillaris FVs was based on a 20-µm slab of imaged tissue, the exact location of which is likely to vary among individuals. A third limitation is that the main factor influencing the calculation of CVIs is image quality, which determines the ability to identify the choroid–scleral interface. The relatively high resolution and contrast of our images yielded good repeatability for choroidal segmentation. Although we attempted to evaluate the topographic characteristics of the alterations in choroidal vascularity by two cross-sectional B-scans, utilization of three-dimensional volumetric OCT data with automated segmentation would allow for more detailed delineation of the choroidal vasculature at different regions and sublayers.

CONCLUSIONS

In conclusion, not only choroidal thickness but also choroidal vascularity and choriocapillaris blood perfusion were lower in the more myopic eyes than in the less myopic eyes of anisomyopic adults. Reduction of the CVI and increases of choriocapillaris FVs correlated positively with the severity of myopia, as well as with choroidal thinning, indicating that ChBF is disturbed in human myopia. Determining the possible causal nature of these associations will require longitudinal research on school-age children, as well as further research in animal models.

References

1. Holden BA, Fricke TR, Wilson DA, et al. Global prevalence of myopia and high myopia and temporal trends from 2000 through 2050. *Ophthalmology.* 2016;123(5):1036–1042.

2. Flitcroft DI. The complex interactions of retinal, optical and environmental factors in myopia aetiology. *Prog Retin Eye Res.* 2012;31(6):622–660.

3. Ruiz-Medrano J, Montero JA, Flores-Moreno I, Arias L, Garcia-Layana A, Ruiz-Moreno JM. Myopic maculopathy: current status and proposal for a new classification and grading system (ATN). *Prog Retin Eye Res.* 2019;69:80–115.

4. Ohno-Matsui K, Jonas JB. Posterior staphyloma in pathologic myopia. *Prog Retin Eye Res.* 2019;70:99–109.

5. Naidoo KS, Fricke TR, Frick KD, et al. Potential lost productivity resulting from the global burden of myopia: systematic review, meta-analysis, and modeling. *Ophthalmology.* 2019;126(3):338–346.

6. Wei WB, Xu L, Jonas JB, et al. Subfoveal choroidal thickness: the Beijing Eye Study. *Ophthalmology.* 2013;120(1):175–180.

7. Tan CS, Cheong KX. Macular choroidal thicknesses in healthy adults–relationship with ocular and demographic factors. *Invest Ophthalmol Vis Sci.* 2014;55(10):6452–6458.

8. Read SA, Collins MJ, Vincent SJ, Alonso-Caneiro D. Choroidal thickness in myopic and nonmyopic children assessed with enhanced depth imaging optical coherence tomography. *Invest Ophthalmol Vis Sci.* 2013;54(12):7578–7586.

9. Jin P, Zou H, Zhu J, et al. Choroidal and retinal thickness in children with different refractive status measured by swept-source optical coherence tomography. *Am J Ophthalmol.* 2016;168:164–176.

10. Jin P, Zou H, Xu X, et al. Longitudinal changes in choroidal and retinal thicknesses in children with myopic shift. *Retina.* 2019;39(6):1091–1099.

11. Read SA, Alonso-Caneiro D, Vincent SJ, Collins MJ. Longitudinal changes in choroidal thickness and eye growth in childhood. *Invest Ophthalmol Vis Sci.* 2015;56(5):3103–3112.

12. Xiong S, He X, Zhang B, et al. Changes in choroidal thickness varied by age and refraction in children and adolescents: a 1-year longitudinal study. *Am J Ophthalmol.* 2020;213:46–56.

13. Wallman J, Wildsoet C, Xu A, et al. Moving the retina: choroidal modulation of refractive state. *Vision Res.* 1995;35(1):37–50.

14. Wildsoet C, Wallman J. Choroidal and scleral mechanisms of compensation for spectacle lenses in chicks. *Vision Res.* 1995;35(9):1175–1194.

15. Hung LF, Wallman J, Smith EL. Vision-dependent changes in the choroidal thickness of macaque monkeys. *Invest Ophthalmol Vis Sci.* 2000;41(6):1259–1269.

16. Zhu X, Park TW, Winawer J, Wallman J. In a matter of minutes, the eye can know which way to grow. *Invest Ophthalmol Vis Sci.* 2005;46(7):2238–2241.

17. Shih YF, Fitzgerald ME, Norton TT, Gamlin PD, Hodos W, Reiner A. Reduction in choroidal blood flow occurs in chicks wearing goggles that induce eye growth toward myopia. *Curr Eye Res.* 1993;12(3):219–227.

18. Fitzgerald ME, Wildsoet CF, Reiner A. Temporal relationship of choroidal blood flow and thickness changes during recovery from form deprivation myopia in chicks. *Exp Eye Res.* 2002;74(5):561–570.

19. Zhang S, Zhang G, Zhou X, et al. Changes in choroidal thickness and choroidal blood perfusion in guinea pig myopia. *Invest Ophthalmol Vis Sci.* 2019;60(8):3074–3083.

20. Wu H, Chen W, Zhao F, et al. Scleral hypoxia is a target for myopia control. *Proc Natl Acad Sci USA.* 2018;115(30):E7091–E7100.

21. Ferrara D, Waheed NK, Duker JS. Investigating the choriocapillaris and choroidal vasculature with new optical coherence tomography technologies. *Prog Retin Eye Res.* 2016;52:130–155.

22. Gupta P, Thakku SG, Saw SM, et al. Characterization of choroidal morphologic and vascular features in young men with high myopia using spectral-domain optical coherence tomography. *Am J Ophthalmol.* 2017;177:27–33.

23. Al-Sheikh M, Phasukkijwatana N, Dolz-Marco R, et al. Quantitative OCT angiography of the retinal microvasculature and the choriocapillaris in myopic eyes. *Invest Ophthalmol Vis Sci.* 2017;58(4):2063–2069.

24. Vincent SJ, Collins MJ, Read SA, Carney LG. Myopic anisometropia: ocular characteristics and aetiological considerations. *Clin Exp Optom.* 2014;97(4):291–307.

25. Woodman-Pieterse EC, Read SA, Collins MJ, Alonso-Caneiro D. Regional changes in choroidal thickness associated with accommodation. *Invest Ophthalmol Vis Sci.* 2015;56(11):6414–6422.

26. Chiang ST, Phillips JR, Backhouse S. Effect of retinal image defocus on the thickness of the human choroid. *Ophthalmic Physiol Opt.* 2015;35(4):405–413.

27. Wang D, Chun RK, Liu M, et al. Optical defocus rapidly changes choroidal thickness in schoolchildren. *PLoS One.* 2016;11(8):e0161535.

28. Tan CS, Ouyang Y, Ruiz H, Sadda SR. Diurnal variation of choroidal thickness in normal, healthy subjects measured by spectral domain optical coherence tomography. *Invest Ophthalmol Vis Sci.* 2012;53(1):261–266.

29. Lee SW, Yu SY, Seo KH, Kim ES, Kwak HW. Diurnal variation in choroidal thickness in relation to sex, axial length, and baseline choroidal thickness in healthy Korean subjects. *Retina.* 2014;34(2):385–393.

30. Alonso-Caneiro D, Read SA, Collins MJ. Speckle reduction in optical coherence tomography imaging by affine-motion image registration. *J Biomed Opt.* 2011;16(11):116027.

31. Sonoda S, Sakamoto T, Yamashita T, et al. Luminal and stromal areas of choroid determined by binarization method of optical coherence tomographic images. *Am J Ophthalmol.* 2015;159(6):1123–1131.e1.

32. Agrawal R, Gupta P, Tan K-A, Cheung CMG, Wong T-Y, Cheng C-Y. Choroidal vascularity index as a measure of vascular status of the choroid: measurements in healthy eyes from a population-based study. *Sci Rep.* 2016;6:21090.

33. Zhang Q, Zheng F, Motulsky EH, et al. A novel strategy for quantifying choriocapillaris flow voids using swept-source OCT angiography. *Invest Ophthalmol Vis Sci.* 2018;59(1):203–211.

34. Nickla DL, Wallman J. The multifunctional choroid. *Prog Retin Eye Res.* 2010;29(2):144–168.

35. Zhang L, Lee K, Niemeijer M, Mullins RF, Sonka M, Abràmoff MD. Automated segmentation of the choroid from clinical SD-OCT. *Invest Ophthalmol Vis Sci.* 2012;53(12):7510–7519.

36. Watanabe Y, Takahashi Y, Numazawa H. Graphics processing unit accelerated intensity-based optical coherence tomography angiography using differential frames with real-time motion correction. *J Biomed Opt.* 2014;19(2):021105.

37. Jia Y, Wei E, Wang X, et al. Optical coherence tomography angiography of optic disc perfusion in glaucoma. *Ophthalmology*. 2014;121(7):1322–1332.

38. Fedorov A, Beichel R, Kalpathy-Cramer J, et al. 3D Slicer as an image computing platform for the Quantitative Imaging Network. *Magn Reson Imaging*. 2012;30(9):1323–1341.

39. Mazzaferri J, Beaton L, Hounye G, Sayah DN, Costantino S. Open-source algorithm for automatic choroid segmentation of OCT volume reconstructions. *Sci Rep*. 2017;7:42112.

40. Duan L, Hong Y-J, Yasuno Y. Automated segmentation and characterization of choroidal vessels in high-penetration optical coherence tomography. *Opt Express*. 2013;21(13):15787–15808.

41. Kajić V, Esmaeelpour M, Glittenberg C, et al. Automated three-dimensional choroidal vessel segmentation of 3D 1060 nm OCT retinal data. *Biomed Opt Express*. 2013;4(1):134–150.

42. Spaide RF. Choriocapillaris flow features follow a power law distribution: implications for characterization and mechanisms of disease progression. *Am J Ophthalmol*. 2016;170:58–67.

43. Spaide RF. Choriocapillaris signal voids in maternally inherited diabetes and deafness and in pseudoxanthoma elasticum. *Retina (Philadelphia, Pa.)*. 2017;37(11):2008–2014.

44. Agrawal R, Ding J, Sen P, et al. Exploring choroidal angioarchitecture in health and disease using choroidal vascularity index. *Prog Retin Eye Res*. 2020;77:100829.

45. Li Z, Long W, Hu Y, Zhao W, Zhang W, Yang X. Features of the choroidal structures in myopic children based on image binarization of optical coherence tomography. *Invest Ophthalmol Vis Sci*. 2020;61(4):18.

46. Su L, Ji YS, Tong N, et al. Quantitative assessment of the retinal microvasculature and choriocapillaris in myopic patients using swept-source optical coherence tomography angiography. *Graefes Arch Clin Exp Ophthalmol*. 2020;258(6):1173–1180.

47. Chen Z, Xue F, Zhou J, Qu X, Zhou X. Effects of orthokeratology on choroidal thickness and axial length. *Optom Vis Sci*. 2016;93(9):1064–1071.

48. Hoseini-Yazdi H, Vincent SJ, Collins MJ, Read SA, Alonso-Caneiro D. Wide-field choroidal thickness in myopes and emmetropes. *Sci Rep*. 2019;9(1):3474.

49. Nava DR, Antony B, Zhang LI, Abramoff MD, Wildsoet CF. Novel method using 3-dimensional segmentation in spectral domain-optical coherence tomography imaging in the chick reveals defocus-induced regional and time-sensitive asymmetries in the choroidal thickness. *Vis Neurosci*. 2016;33:E010.

50. Read SA, Fuss JA, Vincent SJ, Collins MJ, Alonso-Caneiro D. Choroidal changes in human myopia: insights from optical coherence tomography imaging. *Clin Exp Optom*. 2019;102(3):270–285.

51. Alshareef RA, Khuthaila MK, Januwada M, Goud A, Ferrara D, Chhablani J. Choroidal vascular analysis in myopic eyes: evidence of foveal medium vessel layer thinning. *Int J Retina Vitreous*. 2017;3:28.

52. Zhao J, Wang YX, Zhang Q, Wei WB, Xu L, Jonas JB. Macular choroidal small-vessel layer, Sattler's layer and Haller's layer thicknesses: the Beijing Eye Study. *Sci Rep*. 2018;8(1):4411.

53. Ravalico G, Pastori G, Crocè M, Toffoli G. Pulsatile ocular blood flow variations with axial length and refractive error. *Ophthalmologica*. 1997;211(5):271–273.

54. Dastiridou AI, Ginis H, Tsilimbaris M, et al. Ocular rigidity, ocular pulse amplitude, and pulsatile ocular blood flow: the effect of axial length. *Invest Ophthalmol Vis Sci*. 2013;54(3):2087–2092.

55. Yang YS, Koh JW. Choroidal blood flow change in eyes with high myopia. *Korean J Ophthalmol*. 2015;29(5):309–314.

56. Wakabayashi T, Ikuno Y. Choroidal filling delay in choroidal neovascularisation due to pathological myopia. *Br J Ophthalmol*. 2010;94(5):611–615.

57. Zhou X, Zhang S, Zhang G, et al. Increased choroidal blood perfusion can inhibit form deprivation myopia in guinea pigs. *Invest Ophthalmol Vis Sci*. 2020;61(13):25.

58. Zhao F, Zhang D, Zhou Q, et al. Scleral HIF-1α is a prominent regulatory candidate for genetic and environmental interactions in human myopia pathogenesis. *EBioMedicine*. 2020;57:102878.